

## Sensorless Parts Orienting with a One-Joint Manipulator

Srinivas Akella  
The Beckman Institute  
University of Illinois  
Urbana-Champaign, IL

Wesley H. Huang  
The Robotics Institute  
Carnegie Mellon University  
Pittsburgh, PA

Kevin M. Lynch  
Biorobotics Division  
Mechanical Engineering Lab  
Tsukuba, Japan

Matthew T. Mason  
The Robotics Institute  
Carnegie Mellon University  
Pittsburgh, PA

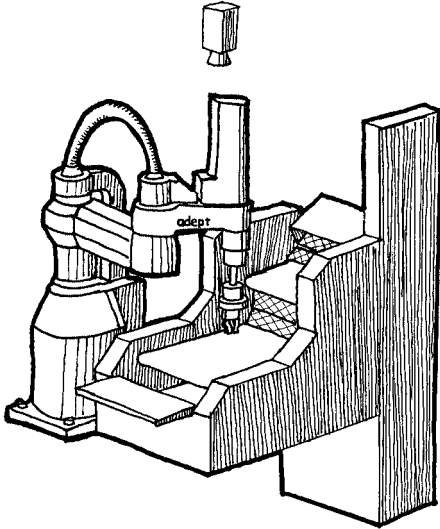


**Figure 1:** The Adept Flex Feeder System. A SCARA robot picks parts off the middle of three conveyors. These three conveyors, along with an elevator bucket, circulate parts; an overhead camera looks down on the back-lit middle conveyor to determine the position and orientation of parts.

### Abstract

*This paper explores a sensorless technique for orienting planar parts. We follow an approach described in earlier papers [3, 4] called 1JOC for One Joint Over Conveyor, which can perform planar manipulation using a single controlled joint in combination with a constant-velocity conveyor. Our previous work demonstrated that the 1JOC approach can orient and feed planar polygonal parts, given a singulated part in a known initial location. This paper shows that a variation called the Sensorless 1JOC can orient and feed polygonal parts up to symmetries in the underlying mechanics, without knowing the initial location and without sensors.*

### 1 Introduction

This paper adopts an approach to planar manipulation called “1JOC” (One Joint Over Conveyor, pronounced “one jock”) [3]. Initially the approach was conceived as a variation on the Adept Flex Feeder (see Figure 1), which is used to feed parts in automated factories. The Flex Feeder uses a system of conveyors to recirculate parts, presenting them in random orientation to a camera and robotic manipulator. Those parts that are in a graspable configuration may then be picked up by the robot and assembled into a product, placed

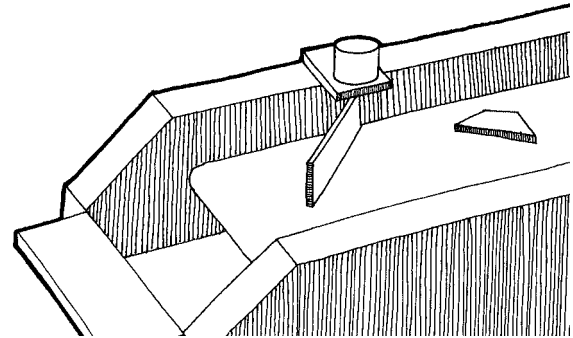


**Figure 2:** The Flex Feeder with a rotatable fence.

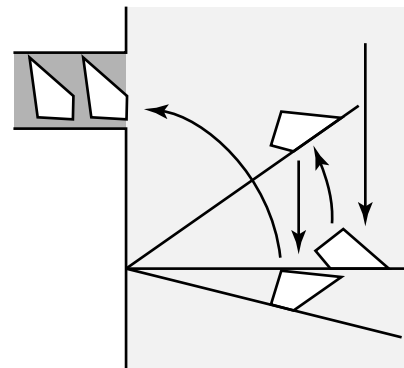


**Figure 3:** We can feed a part by alternately pushing it with the fence and letting it drift along the conveyor.

in a pallet, or otherwise processed.

The question addressed in earlier work is whether, at least in parts feeding applications, we could replace the four-degree-of-freedom robotic manipulator with a simpler single-degree-of-freedom device. Figures 2 and 3 show a simple method using a fence driven by a single revolute joint. By a sequence of pushing operations, punctuated by drift along the conveyor, the fence can move a part from an initially random pose to the entry point of a feeder track which carries the part to the next station.

For the present paper, we have removed the camera which sensed the initial pose of the part, and have made some modifications to the shape and motion of the fence. The resulting system is called the *sensorless 1JOC*. The main result of the present paper is:

The sensorless 1JOC can orient polygons to symmetry in the push function.

Goldberg [14] demonstrated that a sequence of *normal pushes* can orient polygons up to symmetries in the *push function*. We demonstrate a set of sensorless IJOC actions that implement Goldberg’s normal pushes.

We begin by tracing some of the intellectual predecessors (Section 2: Related Work). Then we outline our assumptions, define the primitives, and analyze their behavior (Section 3: Sensorless IJOC Model). Then we describe a planner we implemented (Section 4: Planning). The penultimate section describes our implementation of the sensorless IJOC (Section 5: Implementation). Finally we draw a few conclusions (Section 6: Conclusions).

## 2 Related Work

This paper touches on a number of topics, so that an adequate discussion of our intellectual precedents seems impossible in the space available. The interested reader should refer to [3, 12, 22]. A preliminary description of our work with the sensorless IJOC appeared as [4]. The present paper includes a more complete analysis of the primitives, proof of the necessity of the full  $(-\pi, \pi)$  range of part rotation, a description of the planner, and a more current description of the implementation.

Much of this work was inspired by industrial parts feeders such as bowl feeders and the APOS system (Hitakawa [18]). Related research includes dynamic parts orienting on a vibrating plate (Böhringer *et al.* [8], Swanson *et al.* [33]). Other forms of nonprehensile manipulation are parts orienting by tray-tilting (Erdmann and Mason [13]), tumbling (Sawasaki *et al.* [32]), pivoting (Aiyama *et al.* [2]), tapping (Higuchi [17], Huang *et al.* [19]), two pin manipulation (Abell and Erdmann [1]), and two palm manipulation (Erdmann [12], Zumel and Erdmann [35]).

Much of the work on underactuated manipulation has exploited dynamic coupling among freedoms. Research on underactuated manipulators includes that of Oriolo and Nakamura [29] and Arai and Tachi [6]. Arai and Khatib [5] demonstrated rolling of a cube on a paddle held by a PUMA. Their motion strategy was hand-crafted with the assumption of infinite friction at the rolling contact. In work closely related to the work reported here, Lynch and Mason [25, 22, 23] report automatic planning of rolling, throwing, and snatching tasks using a single degree of freedom robot. A good introduction to nonlinear control is given by Nijmeijer and van der Schaft [28], and nonholonomic robotic systems are discussed in the texts by Latombe [20] and Murray *et al.* [27].

Work on orienting parts using the task mechanics, with and without sensing, goes back to Grossman and Blasgen [16], whose system brought objects to a finite number of orientations in a tilted tray, where their orientation was determined by a tactile probe. Erdmann and Mason [13] developed an automatic sensorless tray tilting system based on the task mechanics. Peshkin and Sanderson [30] used results on the motion of a pushed object to find a sequence of fences to automatically orient a sliding part. Brokowski, Peshkin, and Goldberg [9] designed curved fence sections to eliminate

uncertainty in the orientations of parts being oriented by the fences. Goldberg [14] developed a backchaining algorithm to orient polygonal parts up to symmetry using a frictionless parallel-jaw gripper. Wiegley *et al.* [34] developed a complete algorithm to find the shortest sequence of frictionless curved fences to orient a polygonal part.

Minimalism in robotics has also been studied by Donald *et al.* [11], Canny and Goldberg [10], and Böhringer *et al.* [7]. Raibert [31] and McGeer [26] constructed simple, elegant machines that use dynamics for stable locomotion.

## 3 Sensorless IJOC Model

This section describes the sensorless IJOC, defines the primitive actions employed, and addresses the main issue, which is the system’s ability to orient polygons. The main argument is to show that we can use the sensorless IJOC to implement Goldberg’s *normal push* actions [14]. It follows that the sensorless IJOC can orient polygons up to symmetry in the push function.

We adopt some conventions to simplify the presentation. We assume an origin at the center of the fence, and we assume the belt’s velocity  $v$  is in the  $-y$  direction. The fence angle is measured with respect to the  $x$  axis. We also have a part frame  $\mathcal{F}_p$  fixed to the part. The fence is finite length, and has a “stop” at each end (see Figure 4). The pivot is not a simple revolute joint. Rather, the fence rolls without slipping on a circle, so that each point on the fence follows an evolute. If this pivot circle has radius  $r$ , then when the fence has rotated 180 degrees CW (CCW), it will also have moved up the belt by  $2r$  and to the left (right) by  $\pi r$ . Moving up the belt by  $2r$  gives the space necessary for the fence to push a part to 180 degrees, release it, and then rotate back to 0 degrees and catch the part as it drifts down the conveyor.

We assume the fence is frictionless. The part is a rigid polygon, of known shape and with a known center of mass. We assume Coulomb’s law applies to the contact between polygon and conveyor, with a uniform coefficient of friction. (The *center of friction* is therefore coincident with the center of mass.) We also assume quasistatic mechanics, so that the motion of the part is determined by a balance among contact forces and gravity.

The analysis depends on the definitions of *stable edge* and *metastable edge*. An edge of a polygon is a *stable edge* if the perpendicular projection of the center of friction to the edge is in the interior of the edge segment. An edge of a polygon is a *metastable edge* if the center of friction projects to a vertex. Note that when the fence is held horizontal, *i.e.* at zero degrees, a part resting on a stable edge will be stable. Metastable edges will require special treatment.

### 3.1 Primitives

There are three primitives for sensorless orienting of polygons: the *catch*, the *tilt*, and the *stable push* (see Figure 5):

- A *catch* begins with the part either above or on the fence. The fence is held at zero degrees until the part settles to a stable orientation on the fence.

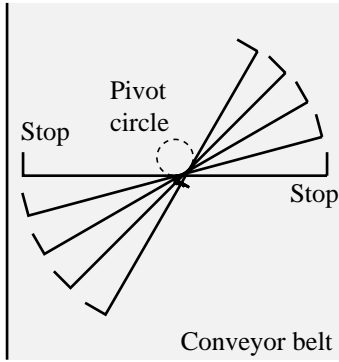


**Figure 4:** The sensorless 1JOC.

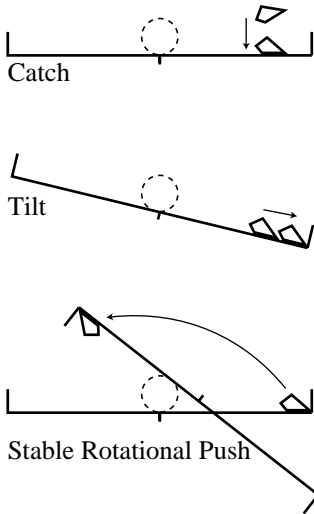


**Figure 5:** Primitives used for sensorless orienting.

- A *tilt* begins with the fence horizontal and the part resting on a stable edge. The fence is then tilted slightly CW (CCW) and the part slides without rolling to the right (left) stop.
- A *stable push* begins with the part on a stable edge at the left stop for a CW push, or at the right stop for a CCW push. The fence rotates, pushing the part, so that the part remains fixed relative to the fence.

We consider each primitive in detail to show that they behave as described above.

### 3.1.1 The Catch

A catch occurs when a part on the conveyor contacts the fence held stationary at 0 degrees and rotates onto a stable edge.

There are a few subtleties that must be addressed:

- *Convergence time.* How long must the system wait for the part to converge to a stable edge? We need an upper bound on convergence time. In principle this upper bound can be obtained using Peshkin's and Sanderson's results [30]. However there is an exception, which occurs when a part is balanced on a vertex with its cen-

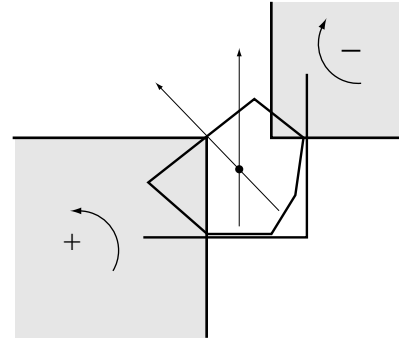


**Figure 6:** The maximum tilt angle can be derived using simple force-torque balance. Here the constraints are represented using moment-labeling regions (Mason [24]). The convex combination of the contact forces consists of the set of all forces that yield positive moment about the region labeled + and negative moment about the region labeled -. Two forces are shown—the force required for a tilt angle of zero, and a force which just begins to violate the constraint, defining the maximum tilt angle. A non-zero maximum always exists, because the polygon is on a stable edge.

ter of friction directly above. Our planning method will avoid these configurations, but there are two special cases discussed below.

- *Starting configuration.* If we start with an unoriented polygon above the fence, the part could arrive balanced on a vertex, or very nearly balanced. In that case there is no upper bound on convergence time. The easiest way to deal with it theoretically is to assume the part starts on the fence on a stable edge, i.e., just after the initial catch. The easiest way to deal with it practically is to determine a time that allows convergence with a very high probability.
- *Metastable edges.* Convergence time is also unbounded for a metastable edge. We need some method of perturbing the fence so that the polygon does not linger indefinitely on a metastable edge. It turns out that a very small rotation of the fence, opposite to the desired part rotation, moves the contact normal off of the center of gravity, inducing a torque that causes the desired part rotation.
- *Stop interference.* As a part converges to a stable edge, it may come into contact with a stop, following a very small stable push. We know of no instance where this possibility affects the success of the plan, and we will simply assume that it is not a problem.

### 3.1.2 The Tilt

A tilt is a CW or CCW rotation of the fence so that a part resting on a stable edge on the fence at 0 degrees slides without rotating to the right or left stop. The sensorless 1JOC uses a tilt before each stable push, and once more at the end to eliminate positional uncertainty of the part.

The part slides faster for steeper tilts, but there is a limit to how steep we can tilt the fence without rotating the part when it contacts the stop. Figure 6 illustrates a simple way of determining the maximum tilt angle.

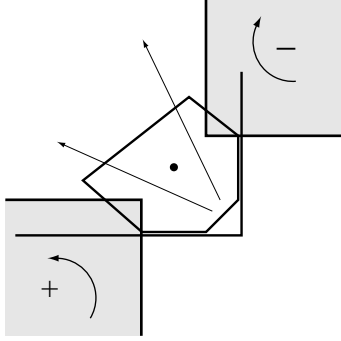


**Figure 7:** Frictionless contact forces through the edges can be represented as moment-labeling regions as in Figure 6.

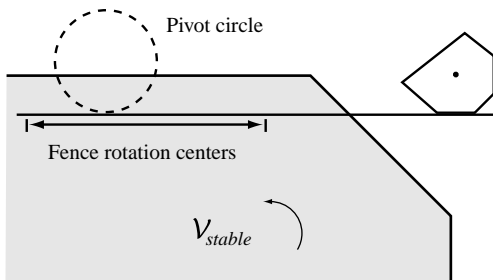


**Figure 8:** The set of CCW stable pushing motions  $\mathcal{V}_{stable}$  represented as rotation centers. Also shown is an example pivot circle and the points on the fence that roll on the pivot circle as it rotates from  $-\pi/2$  to  $\pi$ .

### 3.1.3 The Stable Push

When the part is resting against the right (left) fence stop, a stable push allows the fence to rotate the part CCW (CW). The part remains fixed relative to the fence as it moves. To show that these pushes are stable, we must ensure that the contact forces provided by the fence and the stop can balance the support friction force for any pressure distribution of the part consistent with the center of friction. In this section we show that it is always possible to choose a pivot circle radius  $r$ , fence length, and ratio of the conveyor velocity  $v$  to the fence's pushing angular velocity  $\omega$  to make the pushes stable.

Assume the part is resting against the right stop. The set of possible contact forces is given by the convex combination of the frictionless forces at each contact (Figure 7). For a set of contact forces, we can find a set of stable pushing motions using the method described in (Lynch [21]). Figure 8 shows the CCW stable pushing motions  $\mathcal{V}_{stable}$  for the example of Figure 7. The stable pushing motions are represented as rotation centers fixed in the part frame  $\mathcal{F}_p$ , relative to the conveyor it is sliding on. For these rotation centers, the contact forces can balance the support friction force for any pressure distribution of the part.<sup>1</sup>

Now we assume that the conveyor velocity  $v$  is negligible. Then during a stable push, the rotation center in the part frame  $\mathcal{F}_p$  is the point on the fence in contact with the

<sup>1</sup>Technically, to prove the motion is stable, we must also prove that no other motions of the part are possible. Here we simply assume it to be the case.

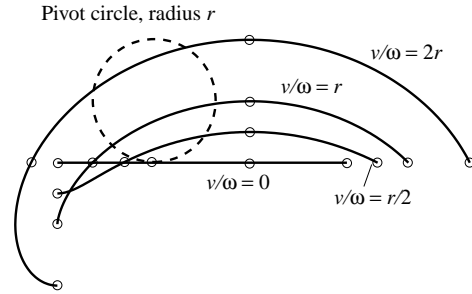


**Figure 9:** Curves of the rotation center of the part relative to the conveyor during stable pushing. The curves shown are for several different ratios of  $v/\omega$ . Each curve is drawn by varying the fence angle  $\theta$  in the range  $[-\pi/2, \pi]$ . Circles are drawn around the rotation centers on each curve at fence angles  $-\pi/2, 0, \pi/2, \pi$ .

pivot circle. Defining the zero location on the fence to be the point in contact with the circle when the fence is held at zero degrees, the rotation centers on the fence sweep the range  $-r\pi/2$  to  $r\pi$ , where  $r$  is the radius of the pivot circle, as the fence rotates from  $-\pi/2$  to  $\pi$ . (Note that  $-\pi/2$  is the steepest possible tilt angle.) We can see in the example of Figure 8 that the push is stable for all angles of the fence.

We can always choose the fence to be long enough that the push is stable for all fence angles. When the rotation center is an infinite distance away along the fence, the required contact force  $\mathbf{f}$  is normal to the fence and through the center of friction. As the rotation center moves in along the fence, the required contact force smoothly rotates counterclockwise because the part's support friction is "above" the fence. This counterclockwise force is provided by the stop (see Figure 7). More precisely, we can define the largest ball  $\mathcal{B}$  of forces about  $\mathbf{f}$  such that all forces in  $\mathcal{B}$  and counterclockwise of  $\mathbf{f}$  can be provided by the contacts. Because  $\mathcal{B}$  always has nonzero radius, the distance to the nearest stable rotation center is finite, implying that we can always choose a sufficiently long fence to make pushing stable if the conveyor velocity  $v$  is negligible.

If the conveyor velocity  $v$  is not negligible with respect to the pushing angular velocity  $\omega$ , the rotation center of the part relative to the conveyor during stable pushing can be written as a function of the ratio  $v/\omega$ . For a fence angle  $\theta$ , the rotation center location is  $(x, y)$ ,  $x = \theta r + \frac{v}{\omega} \cos(\pi - \theta)$ ,  $y = \frac{v}{\omega} \sin(\pi - \theta)$ , where the  $x$  axis is aligned with the fence and the origin is the point on the fence in contact with the pivot circle at  $\theta = 0$ . The rotation center traces out a curve in the part frame  $\mathcal{F}_p$  (Figure 9).

For a push to be stable, the curve must stay inside  $\mathcal{V}_{stable}$ . For a given pivot circle, fence length, and pushing velocity  $\omega$  (perhaps limited by the quasistatic assumption), we would like to find the highest possible conveyor velocity  $v$ . To do this, we increase  $v$  until the curve no longer remains in  $\mathcal{V}_{stable}$  (Figure 10). By doing this for each possible configuration of a given part, we can find a maximum conveyor velocity guaranteed to give stable pushes for all configurations. Maximizing the conveyor speed maximizes the feeder's throughput.

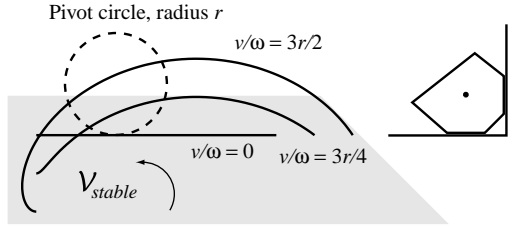


**Figure 10:** Rotation center curves for different ratios  $v/\omega$ . For this example, the maximum conveyor velocity  $v$  that guarantees stable pushes is  $3r\omega/4$ . For larger values, the curve leaves  $\mathcal{V}_{stable}$ .

## 4 Planning

The sensorless 1JOC can use the primitives described above to orient parts sensorlessly. A sensorless orienting plan begins with a catch to acquire the part, followed by a sequence of stages to bring a known part edge to rest on the fence. Each stage consists of a tilt, a stable push, and a catch. The final step of the plan is a tilt to bring the part to a known stop of the fence. At the end of plan execution, the part is in a known orientation at a known position on the fence.

### 4.1 Predicting Part Rotation

The fence can rotate a part by any angle in the range  $[0, 2\pi)$  using a stable push. Each stable push is followed by a catch when the part drifts into contact with the fence. Viewed from a frame fixed in the belt, each catch is a *linear normal push*, meaning that the fence is pushing the part in a direction normal to the fence face. To determine the rotation of the part during a catch, we follow Goldberg [14] in using the *radius function* (Figure 11). The radius of a part is the perpendicular distance from a reference point in the part to a supporting line. The radius function  $r : \mathcal{S}^1 \rightarrow \mathcal{R}^1$  is a plot of the radius as the supporting line is rotated, and has a period of  $2\pi$ . When the center of friction is the reference point and the fence is the supporting line, the local minima of the radius function occur at stable edges of the part. A part being pushed by a fence rotates to achieve a minimum radius. Each local minimum in the radius function determines a convergent orientation, and each local maximum determines a divergent orientation. Hence a normal push has the net effect of mapping the entire interval between two divergent orientations to the enclosed convergent orientation.

The *push function* [14], obtained from the radius function, is an alternative representation of the effect of a normal push. It is a mapping  $p : \mathcal{S}^1 \rightarrow \mathcal{S}^1$  from the initial relative orientation of a part to the resulting orientation (Figure 12), and has a period of  $2\pi$ . Symmetry in part shape with respect to the center of friction leads to a period less than  $2\pi$ , and we say the part has a symmetric push function.

A compact representation of the push function is shown in Figure 13.

### 4.2 Plan Existence and Generation

The push function is a monotonic step function which wraps around at  $2\pi$ . This means that Goldberg's backchaining algorithm [14] can be used to find the shortest sequence of fence rotations to orient a part. Orienting a part with  $n$

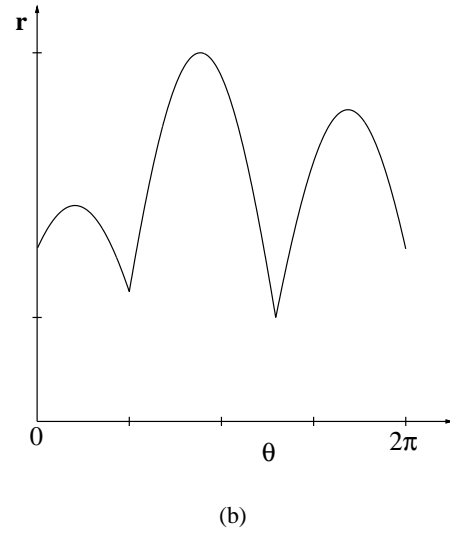
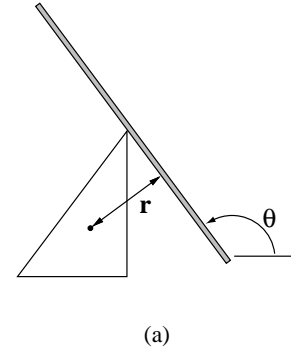


**Figure 11:** The radius function for a triangle with its center of friction indicated by the black dot. (a) The radius  $r$  of a part at a fence orientation  $\theta$  is the perpendicular distance from the center of friction to the fence. (b) The radius function is the plot of the part radius as the fence orientation is varied. Based on [14].

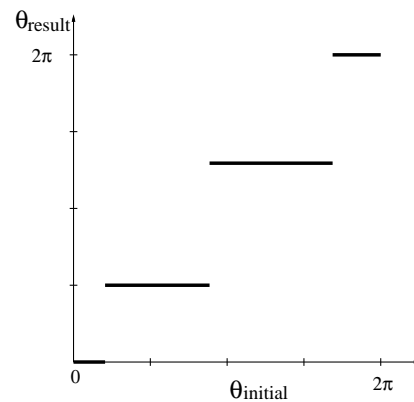


**Figure 12:** The push function for the triangle. The horizontal and vertical axes are the initial and resulting relative orientations of the part.

stable edges takes  $O(n)$  stages. Further, the algorithm can generate a sequence of rotations to orient any part up to symmetry in its push function.

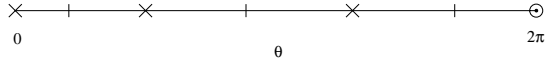


**Figure 13:** A compact representation of the push function for the triangle. The x's and the vertical bars indicate the convergent and divergent fence orientations respectively, and the circle indicates wraparound at  $2\pi$ .

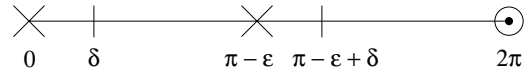


**Figure 15:** This push function requires the fence to push the part at least  $\pi - \delta - \epsilon$  radians before releasing it and catching it. This allows the fence to change its orientation relative to the part by an angle  $-\pi + \delta + \epsilon$ , the minimum required to distinguish between the two stable edges.

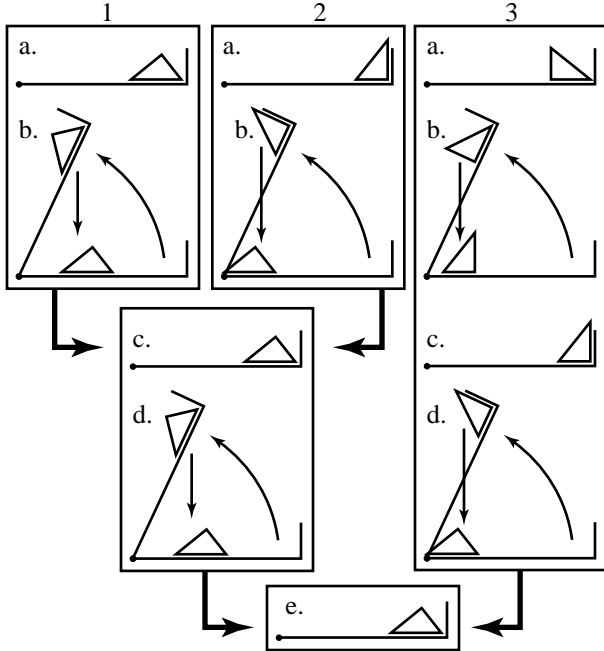


**Figure 14:** Example sensorless feeding plan. Three different initial orientations converge to a single final orientation. The tilts are not shown, and only the right half of the sensorless 1JOC is used in this plan.

In our implementation, we use breadth-first search in the space of representative actions to find the shortest sequence of fence rotations to orient the part. We use the push function to find equivalence classes of actions—action ranges with the same effect. The representative actions chosen from the middle of each range provide a finite discretization of the action space that also covers it. See Figure 14 for an example plan.

The sequence of fence rotations specifies the sequence of stable pushes, each of which is followed by a catch. Stable pushes in the range  $(-\pi, \pi)$  are sufficient to rotate the parts as desired. We have to precede each stable push with an appropriate tilt. Prior to a CCW stable push in the range  $[0, \pi)$ , we tilt the fence CW to bring the part to the right stop. Prior to a CW stable push in the range  $(-\pi, 0]$ , we tilt the fence CCW to bring the part to the left stop. Once the tilt direction is determined, the tilt angle is computed for the set of possible part orientations for the stage.

To ensure that the sensorless 1JOC can orient all parts up to symmetry in the push function, the fence must be capable of stable pushing anywhere in the range  $(-\pi, \pi)$  before releasing and catching. To see that this is necessary, consider the push function of Figure 15. There are two stable edges at angles  $0$  and  $\pi - \epsilon$ , where  $\epsilon$  is a small positive value, so the

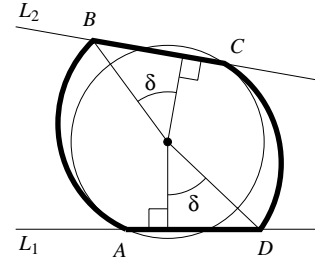


**Figure 16:** Constructing a polygon with the push function of Figure 15. Start with a circle centered at the center of friction of the part. Cut the bottom of the circle with the horizontal line  $L_1$ , and cut the top of the circle with the line  $L_2$ , which is at an angle  $-\epsilon$  to the horizontal. The intersections of these lines with the circle define the points  $A$  and  $C$  as shown. Draw the normals to  $L_1$  and  $L_2$  which pass through the center of friction. Pivot these normals an angle  $\delta$  about the center of friction and intersect them with the lines  $L_1$  and  $L_2$ , giving the points  $B$  and  $D$  as shown. Now construct a curve from  $A$  to  $B$  which spirals away from the center of friction. Construct a similar curve between  $C$  and  $D$ . The part is defined by the curve from  $A$  to  $B$ , the stable edge from  $B$  to  $C$ , the curve from  $C$  to  $D$ , and the stable edge from  $D$  to  $A$ . By making the cuts,  $\epsilon$ , and  $\delta$  arbitrarily small and replacing the curves with an arbitrarily large number of line segments (none of these edges is stable), we create a polygonal part that requires a stable push of up to  $\pi$  to orient it.

push function is not symmetric. The angle range from both stable angles to the counterclockwise limits of their convergence regions is  $\delta$ , where  $\delta$  is a small positive value.

Because the distances to both counterclockwise limits are equal, we must distinguish between the stable edges by using the different distances to their clockwise limits. The fence must move clockwise relative to the part by a magnitude of at least  $\pi - \delta - \epsilon$ . This implies a counterclockwise stable push (before the release and catch) of the same magnitude. As  $\delta \rightarrow 0$ ,  $\epsilon \rightarrow 0$ , the required push angle approaches  $\pi$ .

Figure 16 constructs a part with the push function of Figure 15, requiring a stable push of up to  $\pi$  to orient it. The reflection of this part requires a stable push of up to  $-\pi$ , indicating that the sensorless 1JOC must be capable of stable pushes in the range  $(-\pi, \pi)$  to orient all parts up to symmetry in the push function.

Most parts can be oriented with an angle range much less than  $(-\pi, \pi)$ , and we are interested in characterizing such parts. For example, it is easy to show that all triangles are orientable using the angle range  $(-\pi/2, \pi/2)$ . There exist quadrilaterals, however, that cannot be oriented up to symmetry using this angle range. Goldberg and Overmars [15] showed that  $(-\pi/2, \pi/2)$  is sufficient if parts possess no “partial” symmetries—the distances from each stable angle to each edge of its convergence range are unique.

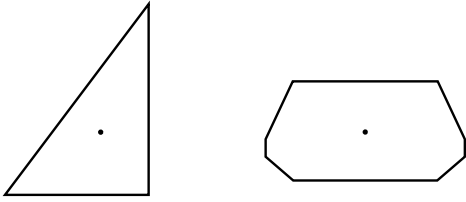


Figure 17: The two test parts used in the experiments.

## 5 Implementation

Our implementation of the sensorless IJOC uses rotation about a fixed pivot point since most parts do not require rotations close to  $\pi$ . We used a plexiglass fence and delrin parts to test the plans. We generated plans to test the right triangle and 8-gon shown in Figure 17. See the two stage plan to orient the triangle in Figure 14. We used a conveyor velocity of 20 mm/sec and fence angular velocities of 30 degrees/sec and 6 degrees/sec for the stable pushes and tilts respectively. We used tilt angles of 45 degrees. The times for catches and tilts to proceed to completion were found empirically. As a practical issue, we note that stable push actions selected from smaller action ranges are less robust than those selected from larger action ranges. In fact, we specify a minimum action range size of 5 degrees for valid actions.

We ran 20 trials for the triangle starting in different configurations along the fence. All 20 trials were successful. We ran 20 trials on the 8-gon for different start configurations, of which 16 were successful. The failures occurred during tilts when the polygon rotated away from the stable edge it was sliding on, probably due to the nonzero friction coefficient of the fence. From our tests on this and other parts, we observed that edges which are nearly unstable sometimes cause undesired part rotations, particularly when a part slides on such an edge during a tilt. Such edges also sometimes require small tilt angles, which may not allow sliding to proceed to completion. Another occasional failure mode occurs when a part contacts the fence stop in the middle of a tilt, leading to undesired part rotation as the tilt progresses.

## 6 Conclusion

This paper demonstrates a system with one controlled degree of freedom that can orient and feed polygons without using sensors. The approach is mechanically simple, yet is readily adapted to new parts, suggesting a possible application in automated manufacturing.

The IJOC approach admits innumerable variations, offering some promise that remaining practical issues (singulation of the part, part feed rate, out of plane motion) may also be resolved.

## Acknowledgments

Many thanks to Costa Nikou and Evan Shechter for implementations of the IJOC on the Adept robot. We thank Mike Erdmann, Garth Zeglin, and Nina Zumel for early discussions about this paper. We thank Adept, NSK, and SONY

for helping us learn about automation and for making equipment available. This work was supported by ARPA and NSF under grant IRI-9318496.

## References

- [1] T. Abell and M. A. Erdmann. Stably supported rotations of a planar polygon with two frictionless contacts. In *IEEE/RSJ International Conference on Intelligent Robots and Systems*, 1995.
- [2] Y. Aiyama, M. Inaba, and H. Inoue. Pivoting: A new method of grasplless manipulation of object by robot fingers. In *IEEE/RSJ International Conference on Intelligent Robots and Systems*, pages 136–143, Yokohama, Japan, 1993.
- [3] S. Akella, W. Huang, K. M. Lynch, and M. T. Mason. Planar manipulation on a conveyor with a one joint robot. In *International Symposium on Robotics Research*, 1995.
- [4] S. Akella, W. Huang, K. M. Lynch, and M. T. Mason. Sensorless parts feeding with a one joint robot. In *Workshop on the Algorithmic Foundations of Robotics*, 1995.
- [5] H. Arai and O. Khatib. Experiments with dynamic skills. In *1994 Japan–USA Symposium on Flexible Automation*, pages 81–84, 1994.
- [6] H. Arai and S. Tachi. Position control system of a two degree of freedom manipulator with a passive joint. *IEEE Transactions on Industrial Electronics*, 38(1):15–20, Feb. 1991.
- [7] K. Böhringer, R. Brown, B. Donald, J. Jennings, and D. Rus. Distributed robotic manipulation: Experiments in minimalism. In *International Symposium on Experimental Robotics*, 1995.
- [8] K. F. Böhringer, V. Bhatt, and K. Y. Goldberg. Sensorless manipulation using transverse vibrations of a plate. In *IEEE International Conference on Robotics and Automation*, pages 1989–1996, 1995.
- [9] M. Brokowski, M. Peshkin, and K. Goldberg. Curved fences for part alignment. In *IEEE International Conference on Robotics and Automation*, pages 3:467–473, Atlanta, GA, 1993.
- [10] J. F. Canny and K. Y. Goldberg. “RISC” industrial robotics: Recent results and open problems. In *IEEE International Conference on Robotics and Automation*, pages 1951–1958, 1994.
- [11] B. R. Donald, J. Jennings, and D. Rus. Information invariants for cooperating autonomous mobile robots. In *International Symposium on Robotics Research*, Hidden Valley, PA, 1993. Cambridge, Mass: MIT Press.
- [12] M. A. Erdmann. An exploration of nonprehensile two-palm manipulation: Planning and execution. In *International Symposium on Robotics Research*, 1995.
- [13] M. A. Erdmann and M. T. Mason. An exploration of sensorless manipulation. *IEEE Transactions on Robotics and Automation*, 4(4):369–379, Aug. 1988.
- [14] K. Y. Goldberg. Orienting polygonal parts without sensors. *Algorithmica*, 10:201–225, 1993.
- [15] K. Y. Goldberg and M. Overmars. Personal communication, 1996.
- [16] D. D. Grossman and M. W. Blasgen. Orienting mechanical parts by computer-controlled manipulator. *IEEE Transactions on Systems, Man, and Cybernetics*, 5(5), September 1975.

- [17] T. Higuchi. Application of electromagnetic impulsive force to precise positioning tools in robot systems. In *International Symposium on Robotics Research*, pages 281–285. Cambridge, Mass: MIT Press, 1985.
- [18] H. Hitakawa. Advanced parts orientation system has wide application. *Assembly Automation*, 8(3):147–150, 1988.
- [19] W. Huang, E. P. Krotkov, and M. T. Mason. Impulsive manipulation. In *IEEE International Conference on Robotics and Automation*, pages 120–125, 1995.
- [20] J.-C. Latombe. *Robot Motion Planning*. Kluwer Academic Publishers, 1991.
- [21] K. M. Lynch. The mechanics of fine manipulation by pushing. In *IEEE International Conference on Robotics and Automation*, pages 2269–2276, Nice, France, 1992.
- [22] K. M. Lynch. *Nonprehensile Robotic Manipulation: Controllability and Planning*. PhD thesis, Carnegie Mellon University, The Robotics Institute, Mar. 1996. Available as CMU-RI-TR-96-05 and at <http://www.cs.cmu.edu/~mlab>.
- [23] K. M. Lynch and M. T. Mason. Dynamic underactuated nonprehensile manipulation. In *IEEE/RSJ International Conference on Intelligent Robots and Systems*, 1996. To appear.
- [24] M. T. Mason. Two graphical methods for planar contact problems. In *IEEE/RSJ International Conference on Intelligent Robots and Systems*, pages 443–448, Osaka, Japan, Nov. 1991.
- [25] M. T. Mason and K. M. Lynch. Dynamic manipulation. In *IEEE/RSJ International Conference on Intelligent Robots and Systems*, pages 152–159, Yokohama, Japan, 1993.
- [26] T. McGeer. Passive dynamic walking. *International Journal of Robotics Research*, 9(2):62–82, 1990.
- [27] R. M. Murray, Z. Li, and S. S. Sastry. *A Mathematical Introduction to Robotic Manipulation*. CRC Press, 1994.
- [28] H. Nijmeijer and A. J. van der Schaft. *Nonlinear Dynamical Control Systems*. Springer-Verlag, 1990.
- [29] G. Oriolo and Y. Nakamura. Control of mechanical systems with second-order nonholonomic constraints: Underactuated manipulators. In *Conference on Decision and Control*, pages 2398–2403, 1991.
- [30] M. A. Peshkin and A. C. Sanderson. Planning robotic manipulation strategies for workpieces that slide. *IEEE Journal of Robotics and Automation*, 4(5):524–531, Oct. 1988.
- [31] M. H. Raibert. *Legged Robots That Balance*. Cambridge: MIT Press, 1986.
- [32] N. Sawasaki, M. Inaba, and H. Inoue. Tumbling objects using a multi-fingered robot. In *Proceedings of the 20th International Symposium on Industrial Robots and Robot Exhibition*, pages 609–616, Tokyo, Japan, 1989.
- [33] P. J. Swanson, R. R. Burrige, and D. E. Koditschek. Global asymptotic stability of a passive juggler: A parts feeding strategy. In *IEEE International Conference on Robotics and Automation*, pages 1983–1988, 1995.
- [34] J. Wiegley, K. Goldberg, M. Peshkin, and M. Brokowski. A complete algorithm for designing passive fences to orient parts. In *IEEE International Conference on Robotics and Automation*, pages 1133–1139, 1996.
- [35] N. B. Zumel and M. A. Erdmann. Balancing of a planar bouncing object. In *IEEE International Conference on Robotics and Automation*, pages 2949–2954, San Diego, CA, 1994.